ISBN: 978-3-95450-247-9 ISSN: 2673-5490 doi: 10.18429/JACoW-IPAC2024-MOPG69

SIMULATIONS OF DIELECTRIC-LINED WAVEGUIDE SEEDING OPTION FOR THZ FEL AT PITZ

X.-Y. Zhang[1,*], X.-K. Li[2], M. Krasilnikov[2], F. Lemery[3], P. Boonpornprasert[2]
[1]Department of Engineering Physics, Tsinghua University, Beijing, China
[2]Deutsches Elektronen-Synchrotron DESY, Platanenallee, Zeuthen, Germany
[3]Deutsches Elektronen-Synchrotron DESY, Notkestraße, Hamburg, Germany

Abstract

The first operational high peak and average power THz self-amplified spontaneous emission (SASE) free electron laser (FEL) at the Photo Injector Test facility at DESY in Zeuthen (PITZ) has demonstrated up to 100 μJ single pulse energy at a center frequency of 3 THz from electron bunches of 2-3 nC. The measured shot-to-shot radiation pulse energy has a fluctuation of 10 %. Shot-to-shot stability and temporal coherence in FELs can be greatly enhanced by the seeding method. In this paper, we propose the use of dielectric-lined waveguides (DLW) to enchance the initial seeding signal. Simulations of using electromagnetic wakefield in DLW to introduce energy modulation to the beam, controlling the conversion between energy modulation and density modulation, and space charge dominated beam matching in the chicane bunch compressor and the undulator will be presented.

INTRODUCTION

High power tunable THz radiation sources are urgently needed for pump-probe experiments at X-ray FELs. Accelerator-based THz radiation sources have the advantages of tunable wavelength, high power, and if driven by the same type photoinjector as the XFELs, can have exactly the same time structure as XFELs, making them ideal radiation sources. A proof-of-principle experiment aiming at such THz sources has been undergoing at PITZ, with the first lasing at a center frequency of 3 THz demonstrated in the summer of 2022 [1] and up to 100 μJ single pulse energy measured from electron bunches of 2-3 nC in following experiments. The gain curve has also been measured and the shot-to-shot radiation pulse energy has a fluctuation of ∼10 %. Preliminary seeding experiments have also been performed using a modulated photocathode laser and have shown earlier saturation and lower pulse energy fluctuation over SASE. While several seeding options have been considered [2], this paper mainly focuses on the beam dynamics of seeding with a DLW. The passive ballistic microbunching experiment using DLW has been done at PITZ in 2017 with a long flattop photocathode laser [3]. In this work, we consider a 2.3 ps root mean squared (RMS) longitudinal gaussian laser instead of flattop laser. Besides, theoretical analysis of the bunching process after DLW is performed. By optimizing the energy-density modulation oscillation, a strong energy modulation is obtained at the chicane entrance, which allows the efficient conversion to density modulation by the chicane.

ENERGY MODULATION BY DLW

There are two DLWs (as shown in Table 1) installed in the PITZ beamline, located at $z = 1.71$ m from the photocathode. In this paper, simulation results with DLW1 is presented; DLW2 results are similar. When the electron beam passes through the DLW, it will excite a wakefield in the DLW, and the wakefield will modulate the longitudinal phase space of the electron beam. The wakefields are computed following the algorithm presented in Ref. [4].

Table 1: DLW parameters

Parameter	**DLW1**	**DLW2**
Inner radius (μm)	450 ± 50	750 ± 50
Outer radius (μm)	550 ± 50	900 ± 50
Length (mm)	50.0 ± 0.1	80.0 ± 0.1
Dielectric constant	4.41	4.41

The strength and cycles of wake potential from an electron bunch moving in the DLW are determined by the charge and current profile of the bunch. In Fig. 1a, the longitudinal electric fields generated by electron bunches of different current profiles (flattop and Gaussian) but the same charge (1 nC) and RMS bunch length (3.85 ps) are compared. The flattop profile generates a significantly stronger modulation than the Gaussian profile, meaning a sharp charge density edge is critical in increasing both the modulation depth and cycles. Taking wake potentials as input for beam dynamics simulations using ASTRA [5], the longitudinal phase spaces after passing the DLW are shown in Fig. 1b and a strong modulation is only observed for the flattop case. In the simulations, the gun phase is set to maximum mean momentum gain (MMMG) phase.

While the upgrade of photocathode laser system is still ongoing, currently only gaussian laser is available. In order to generate a fast rising charge density, very short laser pulses (2.3 ps RMS) are favored. Under the strong and nonlinear longitudinal space charge forces, the electron bunch profile has developed into a quasi-ellipsoidal distribution at the DLW entrance. This can significantly improved the modulation, as shown in Fig. 2. Here, the bunch charge is 1 nC. The gun phase is set to MMMG + 15° to minimize the energy chirp at the DLW. 2 mm laser spot size is chosen.

* xy-zhang20@mails.tsinghua.edu.cn

ISBN: 978-3-95450-247-9 ISSN: 2673-5490 doi: 10.18429/JACoW-IPAC2024-MOPG69

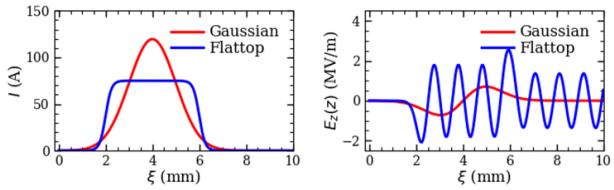

(a) Different current profiles and corresponding wake potentials.

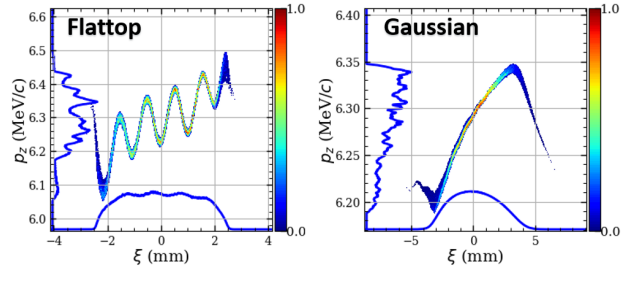

(b) Longitudinal phase spaces after the DLW.

Figure 1: Wake potentials and longitudinal phase spaces of different current profiles.

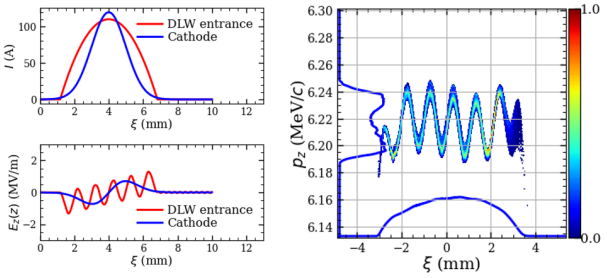

Figure 2: Wake potential (left) and longitudinal phase space (right) of gaussian expansion beam after DLW.

THEORETICAL ANALYSIS OF THE NONLINEAR PHASE SPACE OSCILLATION AFTER DLW

An electron beam with a strong initial density modulation will undergo a nonlinear space charge oscillation (NLSCO) process [6]. The theory can also be applied to a beam with initial longitudinal energy modulation, which allows for better understanding and control of the longitudinal phase space oscillation due to nonlinear space charge forces. Considering a 1D cold fluid model, the system can be written as

$$\partial_t \eta + c\frac{\eta}{\gamma^2}\partial_z \eta = -\frac{eE}{\gamma m_0 c}, \tag{1}$$

$$\partial_z E = -\frac{en_1}{\epsilon_0}, \tag{2}$$

$$\partial_t n + \frac{c}{\gamma^2}\partial_z (n\eta) = 0, \tag{3}$$

where the three unknown functions $n(z,t) = n_0 + n_1(z,t)$, $\eta(z,t) = \Delta\gamma(z,t)/\gamma$, and $E(z,t)$ describe the electron density (n_0 is the average density distribution, $n_1(z,t)$ is modulated density distribution), the energy distribution and the longitudinal space-charge field, respectively. Eq. (1), Eq. (2), Eq. (3) represent the electron motion equation, Poisson's equation, and continuity equation respectively.

For simplicity we assume the initial energy modulation is a cosine modulation, so the initial condition is

$$n(z,0) = n_0, \quad \eta(z,0) = \Delta\eta\cos(kz). \tag{4}$$

where $k = 2\pi/\lambda_k$ represents the modulation wave number. In order to solve these coupled equations, we introduce coordinate transformation and solve it in the Lagrangian coordinate system

$$t = \tau, \quad z = \xi + \int_0^\tau \frac{c\eta(\tau,\xi)}{\gamma^2} d\tau, \tag{5}$$

and the solutions of these equations are

$$n(\xi,t) = \frac{n_0}{1 - \frac{\omega_k}{\omega_b\gamma^2}\Delta\eta\sin(k\xi)\sin(\omega_b t)}, \tag{6}$$

$$\eta(\xi,t) = \Delta\eta\cos(k\xi)\cos(\omega_b t), \tag{7}$$

$$E(\xi,t) = \frac{\gamma m_e c\omega_b}{e}\Delta\eta\cos(k\xi)\sin(\omega_b t), \tag{8}$$

the transformation between the laboratory coordinate system and the Lagrangian coordinate system is

$$kz = k\xi + \Delta\eta\frac{\omega_k}{\omega_b\gamma^2}\sin(\omega_b t)\cos(k\xi). \tag{9}$$

The oscillation frequency is $\omega_b = \omega_p/\gamma^{3/2}$, and $\omega_p = \sqrt{\frac{e^2 n_0}{\epsilon_0 m_0}}$ is known as plasma frequency. When oscillation phase $\omega_b t = \pi/2$, there will be a maximum density modulation

$$(\frac{n}{n_0})_{max} = 1/(1 - \frac{\omega_k\Delta\eta}{\omega_b\gamma^2}), \tag{10}$$

and the energy modulation is zero at that time. By reducing modulation period or increasing modulation depth, a stronger density modulation can be obtained. But these cannot be changed easily under the current experimental conditions. The remaining free parameter is the oscillation frequency, which can be partially tuned by changing the charge density n_0 through focusing and defoscuing.

The solution of Eq. (6) at different oscillation phases are shown in Fig. 3(left) in different colors. From Fig. 2, the modulation depth of $\Delta\eta \approx 3\times10^{-3}$ and wavelength of $\lambda_k \approx 1$ mm can be obtained. Preliminary simulation verification were done by controlling the beam size at a reasonable value with a solenoid after the DLW, and a maximum density modulation at 2.7 meters downstream of the DLW was obtained as shown in Fig. 3(right), with $n/n_0 \approx 1.22$ found at the bunch center. There is a clear quadratic energy chirp due to strong space charge forces and the energy modulation almost disappeared as expected by Eq. (7). The oscillation wavelength λ_p was $4\times2.7 = 10.8$ m in this case. By using the average electron beam size, the oscillation wavelength calculated directly is about 8.49 m. The difference comes from both the non-constant density during the beam transport and non-uniform charge density along the bunch itself. The estimated density modulation from Eq. (10) was 1.26, which agreed well with simulation results.

ISBN: 978-3-95450-247-9 ISSN: 2673-5490 doi: 10.18429/JACoW-IPAC2024-MOPG69

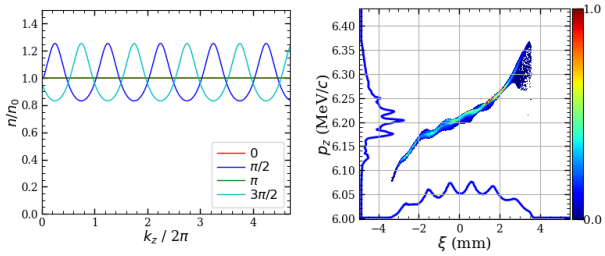

Figure 3: Beam density modulation at different oscillation phases (left) and longitudinal phase space at $\approx \pi/2$ (right).

BEAM TRANSPORT FROM BOOSTER EXIT TO UNDULATOR

The beam dynamics simulations from booster exit to the undulator were performed by OCELOT [7].

A simple idea is to directly transport the electron beam with wished density modulation at the entrance of the undulator. But it turned out that there was almost no density modulation, as shown in Fig. 4(right). This can be explained using the above theory. Since the beam energy increases after passing through the booster, the oscillation frequency decreases. The oscillation wavelength can be estimated by $\lambda_p \approx \sqrt{17^3/6.22^3} \times 10.8 \approx 48.8$ m. The distance from the booster exit to the undulator entrance is about 24 m, corresponding to the phase change by π, which is confirmed by the shift of peaks of energy modulation from booster exit (left in Fig. 4) to the undulator entrance (right in Fig. 4).

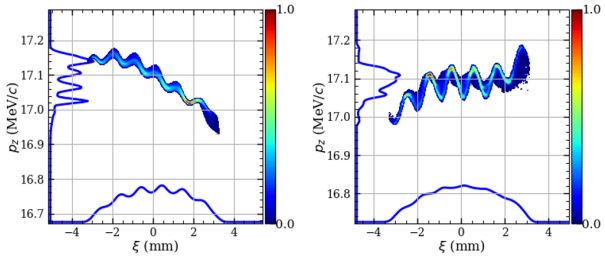

Figure 4: Longitudinal phase space at booster exit (left) and undulator entrance without chicane (right).

In order to maximize the density modulation, the chicane bunch compressor installed in front of the undulator in the PITZ beamline [8] is considered. The ideal case is that the beam is fully energy modulated at the chicane so that the energy modulation can be turned into density modulation completely. However, the chicane is about 10 m upstream the undulator. To make the strongest energy modulation there, one can apply stronger focusing to the electron beam upstream the chicane so the oscillation is faster. In this paper, the focusing was not optimized. Nevertheless, even without this step, the energy modulation was still strong enough to be converted into density modulation, as shown in Fig. 5(left).

In order not to degrade the beam quality in the chicane, the quadrupoles before the chicane have been carefully tuned, using the matching procedure in Ref. [9] to define the matched phase spaces and the Nelder-Mead simplex algorithm to minimize the beam loss in the undulator. The start-to-end beam transport is given in Fig. 6.

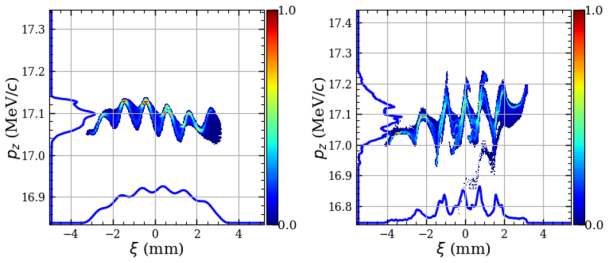

Figure 5: Longitudinal phase space at chicane entrance (left) and undulator entrance with chicane (right).

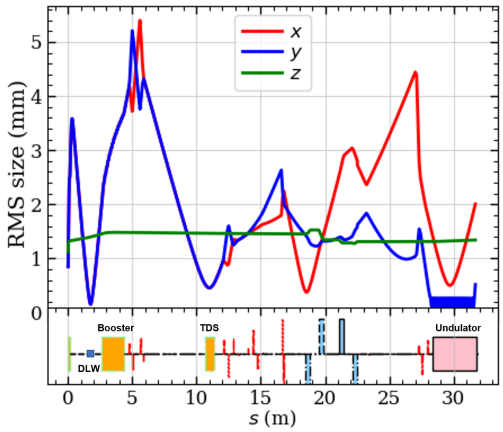

Figure 6: Beam size evolution from start-to-end simulation.

The longitudinal phase spaces at chicane entrance and the undulator entrance are shown in Fig. 5. The chicane rotated the longitudinal phase space so that energy modulation turned into density modulation. However, because R_{56} of the chicane is too strong, it eventually led to over-compression. In the future study, DLW2 in Table 1 will be investigated, since it has a bigger inner radius and thus generates less modulation.

CONCLUSION

Seeding using DLW for the PITZ THz FEL is investigated in this paper, with a focus on generation and optimization of electron beam density modulation. A nonlinear expansion from nonlinear space charge forces is employed to get the maximum energy modulation in the current laser setup and theoretical analysis of the modulation development after DLW is performed. The energy-density-energy modulation oscillation is observed during the beam transport after the booster accelerator, and the chicane is used to convert the energy modulation to density modulation in front of the undulator. In the future, different cathode laser profiles will be investigated and global optimization will be performed with FEL simulations taken into account.

ISBN: 978-3-95450-247-9 ISSN: 2673-5490 doi: 10.18429/JACoW-IPAC2024-MOPG69

REFERENCES

[1] M. Krasilnikov *et al.*, "THz SASE FEL at PITZ: lasing at a wavelength of 100μm", in *Proc. IPAC'23*, Venice, Italy, May 2023, pp. 3948-3951. doi:10.18429/JACoW-IPAC2023-THZG2

[2] G. Georgiev *et al.*, "Simulations of Seeding Options for THz FEL at PITZ", in *Proc. FEL2022*, Trieste, Aug. 2022, pp. 232-235. doi:10.18429/JACoW-FEL2022-TUP40

[3] F. Lemery *et al.*, "Passive Ballistic Microbunching of Nonultrarelativistic Electron Bunches Using Electromagnetic Wakefields in Dielectric-Lined Waveguides", *Phys. Rev. Lett.*, vol. 122, no. 4, pp. 044801, Jan. 2019. doi:10.1103/PhysRevLett.122.044801

[4] M. Rosing and W. Gai, "Longitudinal- and transverse-wakefield effects in dielectric structures", *Phys. Rev. D*, vol. 42, no. 5, pp. 1829–1834, Sep. 1990. doi:10.1103/PhysRevD.42.1829

[5] K. Floettmann, "A Space Charge Tracking Algorithm (ASTRA)", https://www.desy.de/~mpyflo/

[6] P. Musumeci, R. K. Li, and A. Marinelli, "Nonlinear Longitudinal Space Charge Oscillations in Relativistic Electron Beams", *Phys. Rev. Lett.*, vol. 106, no. 18, pp. 184801, May 2011. doi:10.1103/PhysRevLett.106.184801

[7] I. Agapov *et al.*, "OCELOT: A software framework for synchrotron light source and FEL studies", *Nucl. Instrum. Methods Phys. Res., Sect. A*, vol. 768, pp. 151–156, 2014. doi:org/10.1016/j.nima.2014.09.057

[8] A. Lueangaramwong *et al.*, "Commissioning of Bunch Compressor to Compress Space Charge-Dominated Electron Beams for THz Applications", *Appl. Sci.*, 14(5):1982, 2024. doi:10.3390/app14051982.

[9] X. Li *et al.*, "Matching of a Space-Charge Dominated Beam into the Undulator of the THz SASE FEL at PITZ", in *Proc. IPAC'21*, Campinas, Brazil, May 2021, pp. 3244–3247. doi:10.18429/JACoW-IPAC2021-WEPAB257